

Accepted manuscript

Strandberg, R. (2023). Using transfer coefficients to model series-connected multi-junction solar cells with radiative coupling. Applied Physics Letters, 122(25), 1-6.
<https://doi.org/10.1063/5.0152026>

Published in: Applied Physics Letters

DOI: <https://doi.org/10.1063/5.0152026>

AURA: <https://hdl.handle.net/11250/3073399>

Copyright: @ AIP Publishing

This article may be downloaded for personal use only. Any other use requires prior permission of the author and AIP Publishing. This article appeared in Strandberg, R. (2023). Using transfer coefficients to model series-connected multi-junction solar cells with radiative coupling. Applied Physics Letters, 122(25), 1-6. and may be found at <https://doi.org/10.1063/5.0152026>.

Using transfer coefficients to model series-connected multi-junction solar cells with radiative coupling

Rune Strandberg

University of Agder, Department of Engineering Sciences, Jon Lilletuns vei 9, NO-4879 Grimstad, Norway

(*Electronic mail: runes@uia.no)

(Dated: 25 May 2023)

When the quality of multi-junction solar cells becomes sufficiently high, radiative exchange of photons between cells must be included to properly model such devices. In this work it is shown how constants called transfer coefficients can account for radiative coupling in series-connected multi-junction solar cells consisting of several sub-cells which obey the single diode equation. The introduction of the transfer coefficients allows the relation between the voltage and current of the device to be expressed by a convenient closed-form expression that captures the general physics of radiatively coupled multi-junction cells analogous to how the single diode equation describes single-junction solar cells. Another advantage of this model is that it allows the short circuit current and open circuit voltage of radiatively coupled multi-junction cells to be easily calculated. The possibility of extending the model by including some non-idealities is briefly discussed.

In this letter, a model that describes the behavior of optically thick, series-connected multi-junction solar cells is derived. The approach is inspired by the model previously published by Friedman et al.¹, where an inverse JV -characteristic is applied. The starting point of the work in Ref.¹ is the double diode equation, whereas the present work is based on the single diode model. As will be shown, the latter allows the impact of the radiative coupling to be captured by a set of parameters called transfer coefficients whose interpretation is related to observable device parameters. The model may be used to investigate the general behavior of radiatively coupled multi-junction devices in a role similar to that played by the single diode equation for conventional solar cells.

In the traditional single diode model, the individual cells in a series-connected multi-junction device have current densities J_i that follows

$$J_i = J_{G,i} - J_{0,i} e^{\frac{qV_i}{kT}}, \quad (1)$$

when they are operated as single junction cells^{2,3}. $J_{G,i}$ is the generation current density experienced by the cell, $J_{0,i}$ its recombination current density in equilibrium⁴ and V_i is the cell voltage.

When two or more cells are stacked into a series-connected multi-junction device, the device voltage V is the sum of the voltages from the individual cells. If radiative coupling does not occur, inverting the JV -characteristic in Eq. (1) and summing the voltages gives V as a function of the current density J of the stack by⁵

$$V = \sum_i V_i = \frac{kT}{q} \ln \left[\prod_i \frac{J_{G,i} - J}{J_0} \right], \quad (2)$$

which is a special case of the model from Ref.¹. If radiative coupling is present, the JV -characteristic of a top cell in an ideal device can be expressed as⁶

$$J_1 = J_{G,1} - (1 + n^2) J_{0,1} e^{\frac{qV_1}{kT}} + n^2 J_{0,1} e^{\frac{qV_2}{kT}}, \quad (3)$$

where n is the refractive index of the cell material. The value of $J_{0,1}$ is found by integrating over the photon energies that cell 1 may absorb or emit, i.e. from its band gap to infinity⁷. The last term in (3), which accounts for photons emitted from cell 2 to cell 1, is proportional to $J_{0,1}$ because only photons with energy larger than the band gap of cell 1 can be absorbed by the latter. Terms proportional to n^2 are accounting for the radiative coupling between sub-cells, whereas the remaining terms describe interactions with the surroundings. Assuming n to be constant throughout the device, the bottom cell in a stack of N optically thick cells is described by⁶

$$J_N = J_{G,N} - (J'_{0,N} + n^2 J_{0,N-1}) e^{\frac{qV_N}{kT}} + n^2 J_{0,N-1} e^{\frac{qV_{N-1}}{kT}}, \quad (4)$$

if there is a perfect reflector at the back of the device. The remaining cells will follow⁶

$$J_i = J_{G,i} - \left[(1 + n^2) J'_{0,i} + 2n^2 J_{0,i-1} \right] e^{\frac{qV_i}{kT}} + n^2 J_{0,i-1} e^{\frac{qV_{i-1}}{kT}} + n^2 J_{0,i} e^{\frac{qV_{i+1}}{kT}}. \quad (5)$$

The values of $J'_{0,i}$ are found by integrating from the band gap of cell i to the band gap of cell $i-1$ as discussed in Ref.⁶. The terms containing this parameter account for radiation emitted by cell i that cannot be absorbed by cell $i-1$. It holds that $J_{0,i} = J'_{0,i} + J_{0,i-1}$. Since the series-connection dictates that $J_i = J$, for all i , Eqs. (3)-(5) constitutes a set of equations which are linear in the N unknowns $\exp(qV_i/kT)$. From the solutions of this set, the VJ -characteristic can be constructed by

$$V = \frac{kT}{q} \ln \left(\prod_i e^{\frac{qV_i}{kT}} \right) \quad (6)$$

where V_i are functions of J . Reorganizing the solution for a stack of two cells to isolate J , gives the JV -characteristic derived in Ref.⁶. For stacks with more cells, the set of equations

is easily solved numerically. To further explore the behavior of radiatively coupled cells analytically, it is convenient to exploit the fact that in useful devices, practically all the luminescence propagates from cells with higher band gaps to neighboring cells with smaller band gaps, i.e. from cell i to cell $i + 1$. This is true as long as V_i is more than a few times kT larger than V_{i-1} . Since the point of a multi-junction device is to extract the current generated by high energy photons at a higher voltage, this criterion is normally fulfilled for meaningful band gap combinations. Beware, however, that exceptions may exist, for example if the stack has many cells.

When the radiative coupling works in only one direction, we can solve for $\exp(qV_i/kT)$ one cell at the time, starting at the top. Assuming that the band gaps of the sub-cells are sufficiently different allows the approximations $J'_{0,i} \approx J_{0,i}$ and $J_{0,i} \gg J_{0,i-1}$ to be applied – which is done in the following. To generalize the approach, cells or intermittent layers in the stack will be allowed have different refractive indices. n_i is used for the refractive index which limits the transfer of photons to cell i from cell $i - 1$. From the system of equations, the first unknown is found from (3) as

$$e^{\frac{qV_1}{kT}} = \frac{J_{G,1} - J}{(1 + n_1^2)J_{0,1}}. \quad (7)$$

For the next cell, assuming it is not the bottom cell, one arrives at

$$e^{\frac{qV_2}{kT}} = \frac{J_{G,2} - J + \frac{n_2^2}{1+n_2^2}(J_{G,1} - J)}{(1 + n_2^2)J_{0,2}}. \quad (8)$$

For optically thick cells⁸, the quantity $n_2^2/(1 + n_2^2)$ corresponds to the upper limit of the coupling efficiency as described by Steiner and Geisz⁹. This parameter quantifies the fraction of surplus photons transferred from one cell to the next. Eq. (8) can be rewritten by introducing a transfer coefficient T_2 that equals the fraction of the current mismatch $\Delta J_{G,2} = J_{G,1} - J_{G,2}$ which is transferred from cell 1 to cell 2. The result is

$$e^{\frac{qV_2}{kT}} = \frac{J_{G,2} + T_2 \Delta J_{G,2} - J}{(1 - T_2)(1 + n_2^2)J_{0,2}}, \quad (9)$$

where

$$T_2 = \frac{n_2^2}{1 + 2n_2^2} := \mathcal{T}_2. \quad (10)$$

The reason for defining this fraction as both T_2 and \mathcal{T}_2 will become clear below. The numerator in Eq. (9) is now written as the difference between a generation current and the device current as in Eqs. (2) and (7). Proceeding with cells further down the stack, some ink can be saved by defining $\tilde{J}_{0,i} = (1 + n_{i+1}^2)^{1-\delta(N-i)}J_{0,i}$. The Dirac delta function $\delta(N - i)$ appears here since the bottom cell is not emitting luminescence to a cell below. The solution for the remaining cells then becomes

$$e^{\frac{qV_i}{kT}} = \frac{J_{G,i} + T_i \Delta J_{G,i} - J}{(1 - T_i)\tilde{J}_{0,i}} \quad (11)$$

with

$$T_i = \frac{\mathcal{T}_i}{1 + (\mathcal{T}_i - 1)T_{i-1}}, \quad (12)$$

which can be initiated by $T_1 = 0$. The value of \mathcal{T}_i is given by a straightforward generalization of Eq. (10), i.e.

$$\mathcal{T}_i = \frac{n_i^2}{1 + 2n_i^2}. \quad (13)$$

\mathcal{T}_i corresponds to the maximum theoretical coupling factor between neighboring cells as defined by Derkacs et al.¹⁰. $\Delta J_{G,i}$ is a measure of the spectral mismatch of the sub-cells, and given by

$$\Delta J_{G,i} = J_{G,i-1} + T_{i-1} \Delta J_{G,i-1} - J_{G,i} \quad (14)$$

for $i > 1$, whereas $\Delta J_{G,1} := 0$.

The solutions above allow the VJ -characteristic of the entire stack to be conveniently written as

$$V = \frac{kT}{q} \ln \left[\prod_{i=1}^N \frac{J_{G,i} + T_i \Delta J_{G,i} - J}{(1 - T_i)\tilde{J}_{0,i}} \right]. \quad (15)$$

The appearance of T_i in the numerator of Eq. (15) accounts for the part of the radiative coupling that originates from differences in external photon fluxes experienced by the sub-cells. Its presence in the denominator is related to the dark current of the device. By assuming that the voltage is sufficiently high to give $J \gg \max\{J_{0,i}\}$, thermal generation can be ignored, and the dark current is found by setting $J_{G,i}$ and $\Delta J_{G,i}$ to zero in (15). It then becomes clear that $0 < T_i < 1$ leads to an increase in the voltage required by cell i to carry a current density J due to luminescence received from the cell above.

For a perfectly current-matched device, where $J_{G,i} = J_G$, for all i , Eq. (15) can be solved for J , which yields the JV -characteristic

$$J = J_G - \left(\prod_{i=1}^N (1 - T_i)\tilde{J}_{0,i} \right)^{\frac{1}{N}} e^{\frac{qV}{kT}}. \quad (16)$$

This is on the form of the JV -characteristic of a single-junction solar cell with an ideality factor of N . Consequently, expressions for the maximum power point on the form found by Khanna et al.¹¹ for single junction cells, can be applied for this special case, as can textbook expressions for the open circuit voltage. For stacks that are not current matched, the open circuit voltage is easily found by setting $J = 0$ in Eq. (15).

The short circuit current density is found when $V = 0$, which implies that the argument of the logarithm in (15) must equal 1. Since the values of $J_{G,i}$ are several orders of magnitude larger than the values of $J_{0,i}$, the numerator of the factor belonging to the current-limiting cell in Eq. (15) must be so close to zero at short circuit that its small value is negligible. It follows that the short circuit current density is given by

$$J_{sc} = \min\{J_{G,i} + T_i \Delta J_{G,i}\}, \quad (17)$$

which is a concretization of Eq. (10) in Ref.⁹.

The transfer coefficient T_i can thus be interpreted as the fraction of $\Delta J_{G,i}$ that is transferred to cell i at short circuit - provided that cell i is the current limiting cell. Another interpretation can be found if one assumes that the cells above cell i , that is cells 1 to $i - 1$, are current-matched. $\Delta J_{G,j}$ is then zero for $j < i$. If cell i has a generation current $J_{G,i} < J_{G,j}$, T_i will equal the fraction of the difference $J_{G,j} - J_{G,i}$ that is transferred to cell i as a result of the radiative coupling.

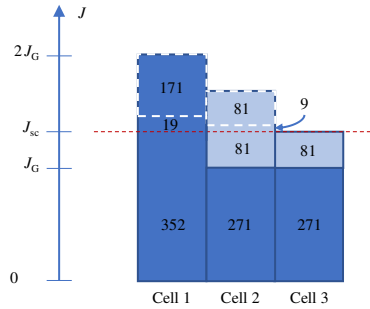


FIG. 1. In this example the middle and bottom cells receive a photon flux equivalent to a generation current density of $J_G = 271 \text{ mA/cm}^2$ from an external light source. The generation current of the top cell is twice as large. The refractive index is set to 3 in this example. After computing the values in Tab. I, the short circuit current-density can be determined which allows the radiative transfer between the cells to be backtracked. The numeric values in the figure show the equivalent current densities, in mA/cm^2 , involved in different processes. The dashed rectangles indicate contributions emitted to the cell below, whereas the lighter color indicates contributions received from the cell above. The fields between the line indicating J_{sc} and the dashed rectangles corresponds to the photons emitted to the surroundings at short circuit.

An example of how the transfer coefficients can be used to track the propagation of the radiative coupling in a stack of three cells is shown in figure 1. Here the middle and bottom cells receive an external generation current density J_G , while the top cell receives a generation current density which is twice as large. Assuming a refractive index of 3 allows the values in Tab. I to be calculated. From the table it becomes clear that the bottom cell is the bottleneck that will limit the short circuit current. If we, for simplicity, assume that $J_G = 271 \text{ mA/cm}^2$, the short circuit current density becomes 352 mA/cm^2 . Consequently, photons corresponding to 81 mA/cm^2 must be radiatively transferred from cell 2 to cell 3. A refractive index of 3 gives a luminescent efficiency of $9/10$, which implies that $1/10$ of the emission from the middle cell, i.e. photons corresponding to 9 mA/cm^2 , is emitted to the surroundings. To assure current-matching, additional photons, equivalent to 81 mA/cm^2 , need to be transferred to the cell in the middle. In total, photons corresponding to 171 mA/cm^2 are thus emitted from the top cell to the middle cell. The top cell should also emit $1/10$ of its total emission, i.e. an equivalent of 19 mA/cm^2 , to the surroundings. This

TABLE I. Parameter values to guide the interpretation of Fig. 1. The refractive index is set to 3 in this example.

Cell	$J_{G,i}$	\mathcal{F}_i	T_i	$\Delta J_{G,i}$	$J_{G,i} + T_i \Delta J_{G,i}$
1	$2J_G$	0	0	0	$2J_G$
2	J_G	$\frac{9}{19}$	$\frac{9}{19}$	J_G	$\frac{28}{19}J_G$
3	J_G	$\frac{9}{19}$	$\frac{171}{271}$	$\frac{9}{19}J_G$	$\frac{352}{271}J_G$

leaves 352 mA/cm^2 in the top cell — exactly what it needs to be current-matched to the other cells.

Introducing the external radiative efficiency (ERE) enables the inclusion of types of non-radiative recombination that gives an ideality factor of 1 into the modeling. The ERE was originally defined for single junction cells as the fraction of the total number of net recombination events that leads to emission of photons from the cell¹². For radiatively coupled cells in a multi-junction stack, it makes sense to slightly redefine the ERE as the fraction of the net recombination events that lead to emission of photons to the surroundings. That is, photons emitted to another cell are not taken into account when calculating the ERE. This assures that a cell of a particular quality will be characterized by the same ERE regardless of whether it is utilized as a single junction cell with a reflector at the back, or as a cell in a multi-junction device radiatively coupled to neighboring cells. This definition of the ERE is in line with the work of Pusch et al.¹³, but differs from the approach of Xia and Krich¹⁴.

The incorporation of the ERE is done by a couple of smaller tweaks. Firstly, non-radiative recombination increases the dark current density, so $\tilde{J}_{0,i}$ must be modified. In accordance with the modified definition of the ERE, $\tilde{J}_{0,i}$ now becomes

$$\tilde{J}_{0,i} = \left(\frac{1}{\text{ERE}_i} + n^2 [1 - \delta(N - i)] \right) J_{0,i} \quad (18)$$

where ERE_i is the ERE of cell i . Secondly, non-radiative recombination reduces the fraction of surplus photons that may be transferred from one cell to another, which leads to smaller transfer coefficients. Using Eq. (18) when deriving the transfer coefficients gives

$$\mathcal{F}_i = \frac{n_i^2}{\frac{1}{\text{ERE}_i} + 2n_i^2}. \quad (19)$$

All other expressions are unaffected by the introduction of non-radiative recombination by means of the ERE.

A combination of a refractive index of 3 and an ERE equal to $1/9$ gives the transfer coefficients $T_2 = 1/3$ and $T_3 = 3/7$. Fig. 2 illustrates the transfer of luminescence throughout a three-cell stack with this combination of parameters when the two upper cells receive a generation current density J_G from an external light source, while the bottom cell receives no external illumination at all. With a luminescent efficiency of $9/10$, 90% of the photons emitted by the top cell will end up in the cell below. For every photon emitted to the surroundings, 8 electron-hole pairs will recombine non-radiatively. Half of

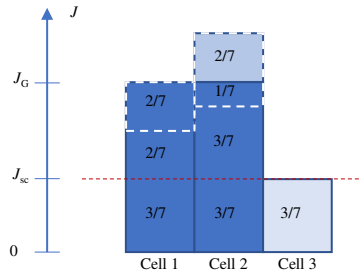


FIG. 2. In this example, cell 1 and cell 2 both have an external generation current density J_G , while cell 3 receives no photons from the external light source. The device is assumed to be short-circuited. Half of the photon surplus absorbed by cell 1 is transferred to cell 2, as marked by the dashed rectangle on the bar of cell 1. Of the remaining half, $1/9$ is emitted to the surroundings and the rest lost through non-radiative recombination. This gives a total generation in cell 2 amounting to $\frac{9}{7}J_G$, where the contribution coming from the top cell is drawn in a lighter color. Cell 2 also emits half of its surplus, the $3/7$ marked by the dashed rectangle, to the cell below. The current-limiting bottom cell thus ends up with a short circuit current equaling $\frac{3}{7}J_G$.

the net recombinations in the top cell will therefore result in transmission of photons to the middle cell. This gives the middle cell an additional generation current density equivalent to $\frac{2}{7}J_G$. The middle cell, having the same ERE and luminescent efficiency as the top cell, will also emit half of its electron surplus to the cell below. The bottom cell thus ends up with a generation current density corresponding to $\frac{3}{7}J_G$, as it should be according to Eq. (17).

The power density of a device can be calculated by multiplying Eq. (15) by J and optimizing the resulting function. Figure 3 shows a plot of the efficiency as a function of the ERE for tandem cells with band gaps of 1.60 and 1.11 eV. The AM1.5G spectrum is used. The solid curves show the efficiency of devices with and without radiative coupling calculated using the model presented in this article. If the ERE is smaller than about 0.1%, the radiative coupling becomes irrelevant. For comparison, dashed curves calculated with a two-diode model resembling that of Friedman et al.¹ are also shown. In the implementation of the two-diode model it is assumed that all non-radiative recombination is taken care of by the second diode. The ERE of the double diode model is then calculated at the maximum power point. The difference between the solid and the corresponding dashed lines is smaller than 0.2 percentage points. In the two-diode model, the ERE is voltage dependent and calculating the ERE at the open circuit voltage, instead of at the MPP, increases the difference by about an order of magnitude due to the different shapes of the JV-characteristics of the two models. The good agreement between the models in Fig. 3 suggests that Eq. (17) may also

give a good approximation of J_{sc} for cells with a two-diode behavior, provided that the ERE at the maximum power point is used. This is indeed the case for the example in Fig. 3, where also the short circuit current density shows a deviation of 0,2% or less between the models.

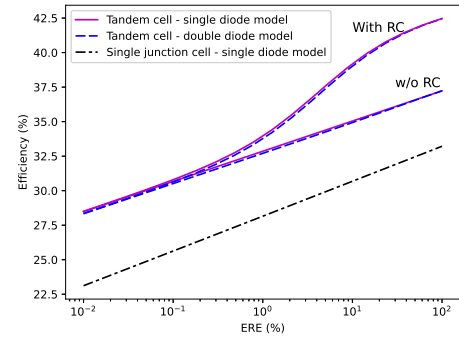


FIG. 3. The efficiency plotted as a function of the ERE for three different cases. The upper pair of curves are calculated for tandems cells with band gaps of 1.60 eV and 1.11 eV with radiative coupling between the cells while the lower pair is calculated without radiative coupling. For each pair, the present model is used for the solid curves, while a double diode model is used for the dashed curves. The curve at the bottom is calculated for a single junction cell with a band gap of 1.11, eV. A refractive index of 3.4 is assumed.

While its ability to give insight into the radiative coupling in stacks with more than two cells is an important strength of the model presented above, a crucial weakness is its inability of incorporating recombination mechanisms that gives ideality factors different from one. The model may therefore be more suited for educational and explorational purposes than for accurate curve fitting of the JV-characteristics of real devices⁹. Some other non-idealities, like reflections or parasitic optical losses in intermediate layers between the cells, may be taken into account by introducing constants at the right instances in the derivation above. Series resistance may be incorporated by adding a term to Eq. (15) as done by Geisz et al.¹⁵, while shunt-resistance is usually negligible in high quality devices¹⁵. Other aspects of real multi-junction devices, like the impact of quasi-Fermi level gradients¹⁶, may be harder to incorporate into the framework presented in this article, but an approach similar to that found in Ref.¹⁵ might be applicable. If the backside of the device is not a perfect reflector, $J_{0,N}$ may be multiplied by a factor between 1 (perfect reflector) and 2 (no reflector).

To summarize, it has been shown that the current-voltage characteristic of ideal radiatively coupled series-connected multi-junction solar cells can be described with a short and handy expression by means of Eq. (15). As an equivalent of the single diode model for multi-junction cells, the model captures the general physics of such cells in the simplest possible

This is the author's peer reviewed, accepted manuscript. However, the online version of record will be different from this version once it has been copyedited and typeset.

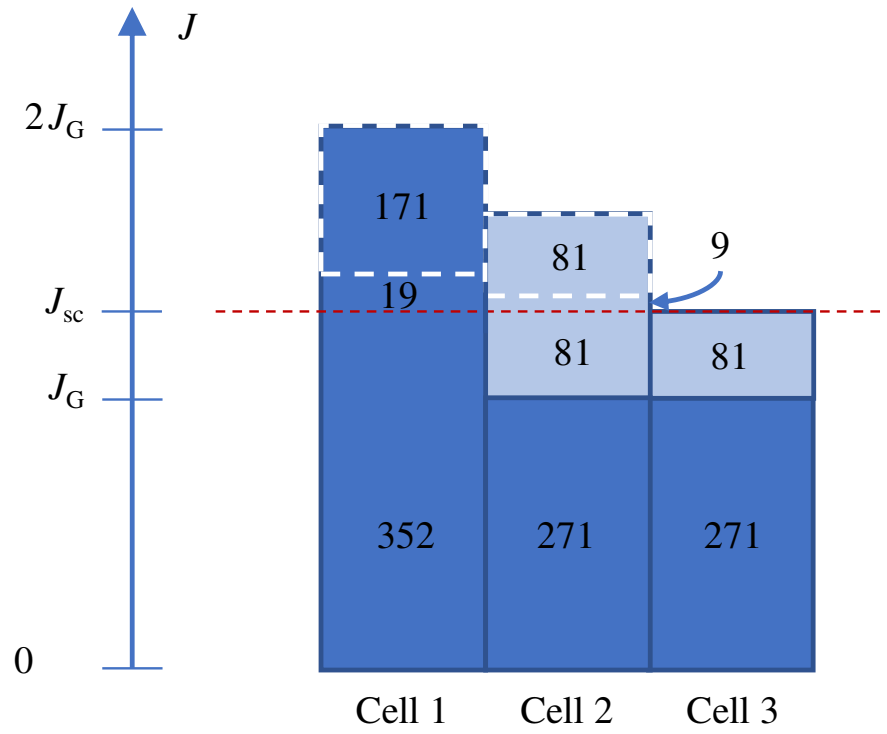
PLEASE CITE THIS ARTICLE AS DOI: 10.1063/1.50152026

way. Some aspects of non-ideal devices may be incorporated into the model, while other may require more extensive models to fully capture the behavior of real cells. The main advantage of the new model is that its simplicity facilitates the interpretability of the radiative coupling.

- ¹D. J. Friedman, J. F. Geisz, and M. A. Steiner, "Analysis of Multijunction Solar Cell Current – Voltage Characteristics in the Presence of Luminescent Coupling," *IEEE Journal of Photovoltaics* **3**, 1429–1436 (2013).
- ²W. Shockley, "The Theory of p-n Junctions in Semiconductors and p-n Junction Transistors," *Bell System Technical Journal* **28**, 435–489 (1949).
- ³W. Shockley and H. J. Queisser, "Detailed Balance Limit of Efficiency of p-n Junction Solar Cells," *Journal of Applied Physics* **32**, 510 (1961).
- ⁴A. Cuevas, "The recombination parameter J_0 ," *Energy Procedia* **55**, 53–62 (2014).
- ⁵E. F. Fernández, G. Siefer, F. Almonacid, A. J. Loureiro, and P. Pérez-Higueras, "A two subcell equivalent solar cell model for III-V triple junction solar cells under spectrum and temperature variations," *Solar Energy* **92**, 221–229 (2013).
- ⁶R. Strandberg, "An Analytic Approach to the Modeling of Multijunction Solar Cells," *IEEE Journal of Photovoltaics* **10**, 1701–1711 (2020), 2001.08553.
- ⁷A. Marti, J. L. Balenzategui, and R. F. Reyna, "Photon recycling and Shockley's diode equation," *Journal of Applied Physics* **82**, 4067–4075 (1997).
- ⁸D. J. Friedman, J. F. Geisz, and M. A. Steiner, "Effect of luminescent coupling on the optimal design of multijunction solar cells," *IEEE Journal of Photovoltaics* **4**, 986–990 (2014).
- ⁹M. A. Steiner and J. F. Geisz, "Non-linear luminescent coupling in series-connected multijunction solar cells," *Applied Physics Letters* **100**, 251106 (2012).
- ¹⁰D. Derkaas, D. T. Bilir, and V. A. Sabnis, "Luminescent coupling in gaas/gainnassb multijunction solar cells," *IEEE Journal of Photovoltaics* **3**, 520–527 (2013).
- ¹¹A. Khanna, T. Mueller, R. A. Stangl, B. Hoex, P. K. Basu, and A. G. Aberle, "A fill factor loss analysis method for silicon wafer solar cells," *IEEE Journal of Photovoltaics* **3**, 1170–1177 (2013).
- ¹²M. A. Green, "Radiative efficiency of state-of-the-art photovoltaic cells," *Progress in Photovoltaics: Research and Applications* **20**, 472–476 (2012).
- ¹³A. Pusch, P. Pearce, and N. J. Ekins-daukes, "Analytical Expressions for the Efficiency Limits of Radiatively Coupled Tandem Solar Cells," *IEEE Journal of Photovoltaics* **9**, 679–687 (2019).
- ¹⁴D. Xia and J. J. Krich, "Efficiency increase in multijunction monochromatic photovoltaic devices due to luminescent coupling," *Journal of Applied Physics* **128**, 013101 (2020), 2004.00081.
- ¹⁵J. F. Geisz, M. A. Steiner, R. M. France, W. E. McMahon, C. R. Osterwald, and D. J. Friedman, "Generalized Optoelectronic Model of Series-Connected Multijunction Solar Cells," *IEEE Journal of Photovoltaics* **5**, 1827–1839 (2015).
- ¹⁶D. Lan, J. F. Geisz, M. A. Steiner, I. Garcia, D. J. Friedman, and M. A. Green, "Improved modeling of photoluminescent and electroluminescent coupling in multijunction solar cells," *Solar Energy Materials and Solar Cells* **143**, 48–51 (2015).

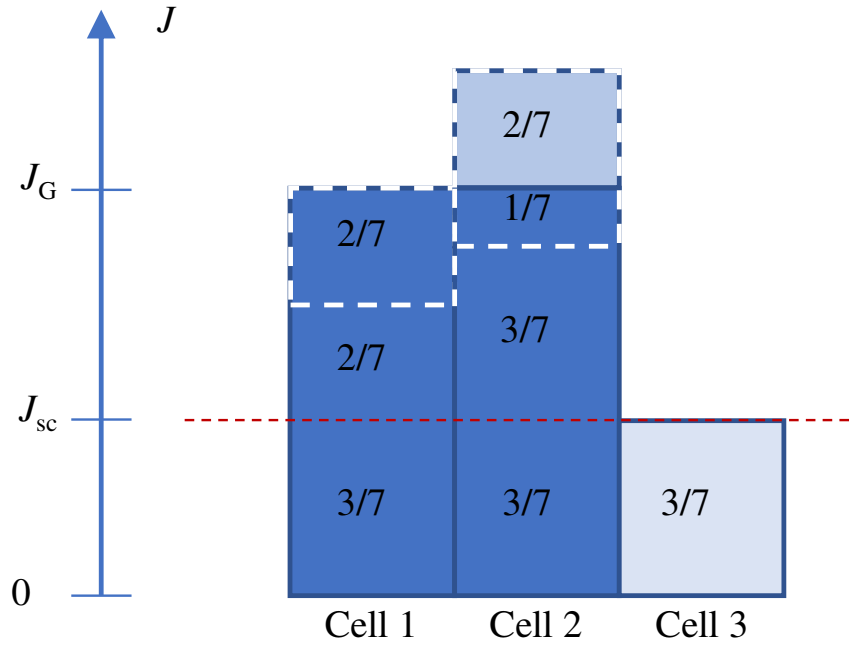
This is the author's peer reviewed, accepted manuscript. However, the online version of record will be different from this version once it has been copyedited and typeset.

PLEASE CITE THIS ARTICLE AS DOI: 10.1063/1.50152026



This is the author's peer reviewed, accepted manuscript. However, the online version of record will be different from this version once it has been copyedited and typeset.

PLEASE CITE THIS ARTICLE AS DOI: 10.1063/5.0152026



This is the author's peer reviewed, accepted manuscript. However, the online version of record will be different from this version once it has been copyedited and typeset.

PLEASE CITE THIS ARTICLE AS DOI: 10.1063/5.0152026

